Energy and angular distributions of the low-energy electron emission in collisions of 4 MeV/*u* bare F ions with He atoms

2012 J. Phys. B: At. Mol. Opt. Phys. 45 225201

(http://iopscience.iop.org/0953-4075/45/22/225201)

J. Phys. B: At. Mol. Opt. Phys. **45** (2012) 225201 (7pp) doi:10.1088/0953-4075/45/22/225201

Energy and angular distributions of the low-energy electron emission in collisions of 4 MeV/*u* bare F ions with He atoms

Deepankar Misra[1], **Aditya H Kelkar**[1], **Pablo D Fainstein**[2] **and Lokesh C Tribedi**[1]

[1] Tata Institute of Fundamental Research, Homi Bhabha Road, Colaba, Mumbai 400 005, India
[2] Centro Atómico Bariloche, Comisión Nacional de Energía Atómica, Avenida E Bustillo 9500, 8400 Bariloche, Argentina

E-mail: dmisra@tifr.res.in and lokesh@tifr.res.in

Received 20 April 2012, in final form 13 September 2012
Published 11 October 2012
Online at stacks.iop.org/JPhysB/45/225201

Abstract
The energy and angular distributions of double-differential cross sections (DDCS) of electron emission from He in collisions with 4 MeV/*u* F^{9+} ions are reported. The derived single-differential distributions and the total cross sections are also reported. The measured distributions of the low-energy electrons between 1 and 400 eV over a wide angular range between 20° and 160° are compared with the state-of-the-art quantum mechanical models. The first Born (B1) and the continuum distorted wave-eikonal initial state (CDW-EIS) approximations are used for this purpose. The DDCS for a given angle was found to fall by a few orders of magnitude over the electron energy range studied. The CDW-EIS model provides excellent agreement with the energy distributions and the angular distributions. The electron energy dependence of the forward–backward asymmetry parameter shows monotonically increasing behaviour. This has been explained very well in terms of the CDW-EIS model, which includes the two-centre effect. A large deviation from the B1 is also observed. We have also derived the single-differential distributions in terms of the angle as well as the electron energy. These distributions are also well reproduced by the CDW-EIS model.

(Some figures may appear in colour only in the online journal)

1. Introduction

Single ionization has been by far the most dominant process in high-energy ion–atom collisions and also has been the subject of considerable studies and discussions since the early days of quantum mechanics [1]. Until the 1950s most experiments were restricted to the measurement of the total ionization cross sections [2]. Kuyatt and Jorgenson [3] carried out the first complete measurements of the angular and the energy dependence of the differential cross sections for electron emission. Up till now, the general method for most of these measurements has been the use of electrostatic analysers, which are placed at various angles relative to the incoming projectile ion beam to study the energy and angular distributions of emitted electrons. However, simultaneous measurement of energy and angular distributions of emitted electrons [4] using the recoil ion momentum spectroscopy technique [5] has been reported in a series of experiments. It has been shown that the shape of the low-energy electron spectrum emitted in heavy-ion–atom collisions is sensitive to various ionization mechanisms such as soft electrons (SE), two-centre electron emission (TCEE), binary encounter (BE) collisions and electron capture to continuum (ECC), which can be identified from the energy and angular distributions of the DDCS spectra [6–20]. In highly charged heavy-ion collisions, the trajectory of the emitted electron is largely affected by the two moving sources of Coulomb potentials, namely the receding highly charged heavy projectile ion and the residual recoil ion. This situation is quite different from the low-charged projective ions, such as e^- and H^+ [21–26]. For the present

collision system, the ratio of the projectile speed to the orbital electron speed, i.e. v_p/v_e, is ~ 9. It has been shown in previous works [6, 12, 13] that even for fast ions, i.e. with the velocity $v_p \gg 1$, the first Born calculation (B1) fails to explain the energy and angular distributions of the ionized electrons. This is because B1 accounts only for the target centre effects and does not consider the effect of the incoming and the outgoing projectile ion on the active electron.

In order to account for both the projectile centre and the target centre effects, a theoretical model based on the continuum-distorted wave-eikonal initial state (CDW-EIS) approximation has been developed by Crothers and McCann [27]. This model has been extended by many workers over the period of time and also for multi-electronic targets [28]. The charge to velocity ratio (perturbation strength), i.e. $q/v \sim 0.7$, is quite large here, and hence, the two-centre mechanism is more applicable here since the distortion of the initial and the final states is appreciable. The helium target atom is a simple two-electron atomic system and is therefore well suited to study the electron-emission mechanisms in ion–atom collisions. In the case of other simple molecules with two electrons, such as H_2, one has to include the mechanism of coherence-driven interference effect [29–35] due to the double-slit nature of the source. This also implies that one has to use a suitable molecular wavefunction for H_2 [36]. It is worth mentioning that the elaborate data sets for angular and energy distributions of fast-ion-induced e-DDCS for a He target are not available for too many cases. For a detailed understanding of the electron-emission mechanisms in terms of different theoretical models, the electron DDCS measurements are required for different projectiles (with atomic number Z) with different velocities (v) in order to have different perturbation strengths. The discrepancy of experimental results and the CDW-EIS model calculations were found to be small for fast-proton projectiles [24] and also for very fast highly charged projectile ions [37]; however, a notable discrepancy in the energy and the angular distributions was always observed for relatively slower and highly charged projectile ions [6, 14, 18, 19]. Since the applicability of the models, based on TCE, depends on Z, V and also the perturbation strength (Z/v), the earlier studies on continuum electron emission cover a limited range of these parameters. To have a comprehensive understanding of the two-centre mechanism more experimental data with different combinations of Z, v and Z/v are required in order to parametrize the TCE. For example, most of the earlier data are on p, He-ions or bare C, or O-ions (except in [37, 6]. This study with bare F ions ($Z = 9$) of energy 76 MeV (i.e. $v \sim$12.7 au) with the perturbation strength 0.70 will suitably complement most of the earlier studies with low-Z ions or a few with high-Z ions. The present measurement, in this sense, will be an important step towards building a wider database and hence towards a better understanding of the mechanisms of two-centre electron emission.

In this paper, we present the details of the measurements of energy and angular distributions of electron DDCS for various emission angles ranging between 20° and 160°. In addition, we report a detailed study of the two-centre effect (TCE) in collisions of 4 MeV/u bare fluorine ions with He by measuring the energy and angular distributions of the DDCS. We have derived the forward–backward asymmetry parameter from the energy distributions, which could be taken as a direct measure of the TCE. The asymmetry parameter has been compared with the CDW-EIS and B1 models. We have also plotted the DDCS ratios for three different angles, where we have compared the DDCS ratios between the data and the B1 calculations with the ratios between CDW-EIS and B1 calculations. The comparison between these two ratios gives a stringent test to the theoretical calculations.

2. Measurements and experimental results

The experiments were carried out for the collision of 4 MeV/u F^{9+} ions with He atoms for electron energy ranging between 1 and 400 eV over an angular range between 20° and 160°. The BARC-TIFR Pelletron accelerator facility in Mumbai was used to obtain the ion beams. The mass-analysed F^{6+} ions were energy analysed by a 90° analysing magnet. The beam was then further stripped using a post-stripper foil assembly [38]. The post-stripped beam was again charge analysed by a switching magnet, and the F^{9+} beam was collimated by two sets of four-jaw slits (2×2 mm^2) placed 1 m apart. The experimental setup has been described earlier [39], and hence, only a short description will be given here. The scattering chamber was flooded with He gas at a static pressure of ~0.1 mTorr for electron energies up to 100 eV and at ~0.3 mTorr for higher energy electrons. This minimizes the scattering of low-energy electrons from the target gas. The electrons emitted from He were energy analysed by a hemispherical electrostatic analyser [39].

3. Comparison with theory

3.1. Energy distributions at fixed angles

Figure 1 shows the measured energy distributions of the DDCS spectra for collision of 4 MeV/u F^{9+} with He atoms. Some of the selected DDCS values are tabulated in table 1. The CDW-EIS and the B1 calculations are shown as the solid and dashed curves, respectively. At each angle, the electrons having energies between 1 and 400 eV were detected for 11 different angles between 20° and 160°. As can be seen from the DDCS spectra, at low energies, ~ few eV, the cross section reaches a maximum due to the contribution from the SE-emission process. These electrons result from very large impact parameter collisions, and hence, the emitted electrons receive very small momentum transfer from the projectile ions. The electrons emitted with energies more than a few tens of eV up to the end of the spectrum (400 eV) result from the so-called two-centre electron-emission (TCEE) process, although there is no clear border line for this definition. The trajectory of these electrons is highly influenced by both the charge centres, namely the residual target ion and the receding projectile ion.

It can be noted that, overall, there is very good agreement with the CDW-EIS model calculations. For intermediate emission energies, good agreement is found, whereas a notable discrepancy has been observed for very low- and high-energy

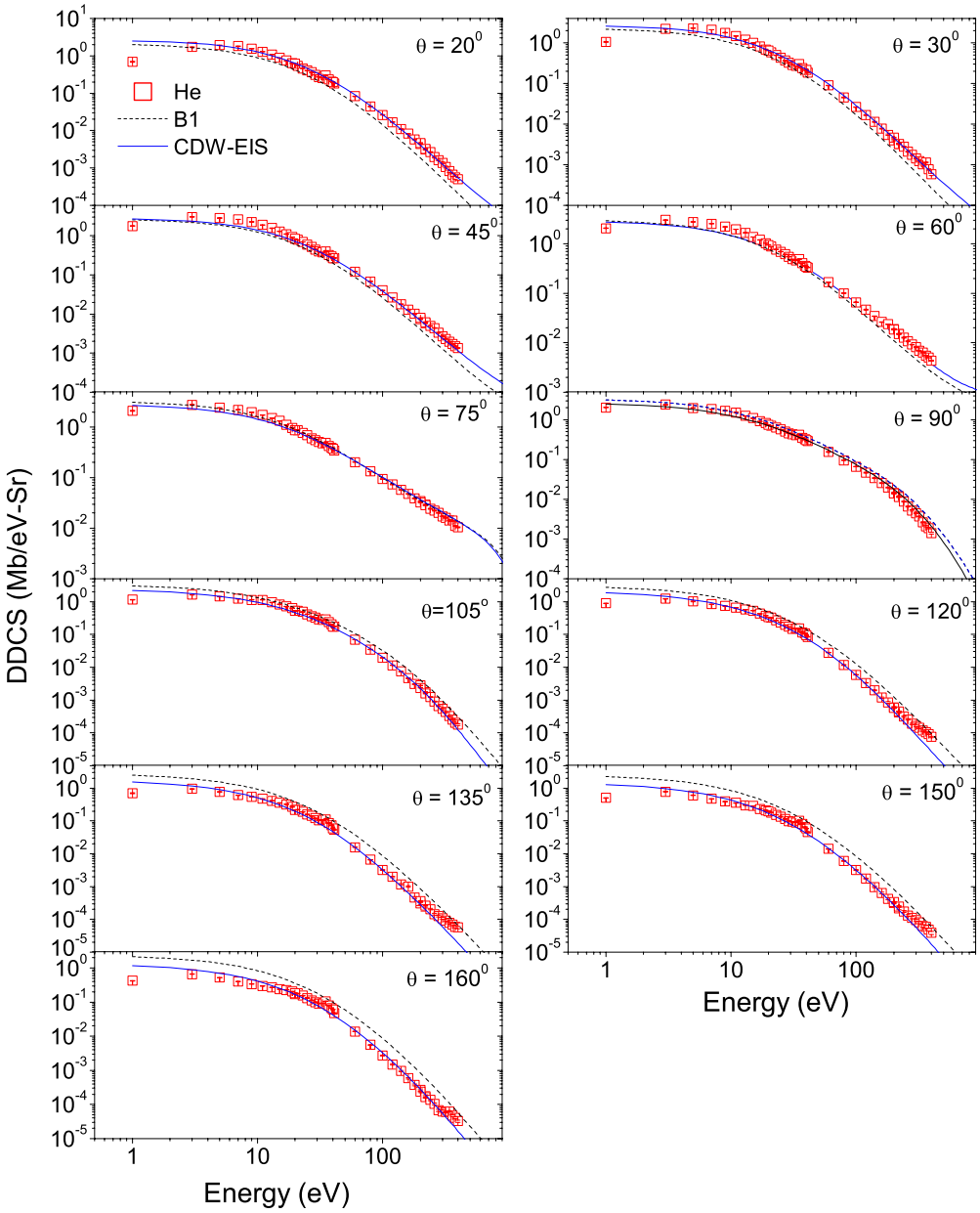

Figure 1. The double-differential cross section of electrons for 11 different angles, namely, 20°, 30°, 45°, 60°, 75°, 90°, 105°, 120°, 135°, 150° and 160°. The CDW-EIS and B1 calculations are shown as the solid and dashed curves, respectively.

electrons and at backward emission angles. In particular, deviations at 1 eV, partially, could be due to the presence of even small stray fields. Also the measured DDCS is found to match quite well with CDW-EIS calculations for angles close to 90°. B1 gives very similar values to CDW-EIS. This may be due to the binary nature of the electron emission and is included in the B1 model, which is a target centre model. However, a slight difference between the CDW-EIS and the B1 can be noted, which may imply the influence of the TCE (or the distortion) even in the case of binary-dominated electron emission. We also derived the single-differential cross sections (SDCSs) as a function of the ejected energy of the emitted electron. Figure 3 shows the SDCS for electron emission from He in collisions with bare F ions. As evident from the figure, the agreement is excellent with the CDW-EIS calculations throughout the whole energy range except for very low-energy electrons where the theory underestimates the data. The B1 calculations also show very good agreement with the experimental cross sections.

In figure 2, we also show the DDCS ratios for 30°, 75° and 150° on a linear scale, in order to provide more closer look at the comparison with the theory. This way one can have a more stringent test of the theory. The experimental cross sections are divided by the B1 calculations and are compared with the theoretical ratios between CDW-EIS and B1 calculations. This ratio gives quantitative information on the deviation from the one-centre model and the applicability of the two-centre model as indicated by earlier workers. As evident from the ratio plots, the agreement is quite good for electron energies ε_e between 20 and 200 eV. However, a discrepancy is observed for very low- and high-energy electrons. The ratio is more than unity and increases with energy for 30°. The overall enhancement

Table 1. DDCS values for collision of 4 MeV/*u* F^{9+} with He in units of Mb/eV sr.

	Angle θ (deg)										
Energy (eV)	20	30	45	60	75	90	105	120	135	150	160
1	6.95E-1	1.06E0	1.77E0	2.06E0	2.09E0	2.00E0	1.15E0	8.90E-1	6.96E-1	5.05E-1	4.26E-1
3	1.71E0	2.20E0	3.02E0	3.06E0	2.76E0	2.40E0	1.63E0	1.22E0	9.56E-1	7.71E-1	6.59E-1
5	1.92E0	2.30E0	2.85E0	2.78E0	2.43E0	1.97E0	1.43E0	1.02E0	7.70E-1	6.01E-1	5.21E-1
7	1.80E0	2.11E0	2.63E0	2.55E0	2.20E0	1.83E0	1.22E0	8.45E-1	6.14E-1	4.77E-1	4.00E-1
9	1.55E0	1.78E0	2.27E0	2.22E0	1.96E0	1.67E0	1.13E0	7.44E-1	5.47E-1	3.90E-1	3.38E-1
11	1.29E0	1.46E0	1.89E0	1.97E0	1.73E0	1.51E0	1.13E0	6.49E-1	4.75E-1	3.58E-1	2.96E-1
13	1.08E0	1.19E0	1.57E0	1.67E0	1.50E0	1.24E0	9.55E-1	5.76E-1	4.10E-1	3.01E-1	2.70E-1
15	8.78E-1	9.98E-1	1.29E0	1.37E0	1.33E0	1.08E0	8.30E-1	5.32E-1	3.54E-1	2.84E-1	2.38E-1
20	6.15E-1	6.48E-1	8.29E-1	9.51E-1	8.69E-1	7.37E-1	5.26E-1	3.34E-1	2.15E-1	1.96E-1	1.80E-1
40	1.98E-1	2.16E-1	2.68E-1	3.47E-1	3.77E-1	3.04E-1	1.75E-1	9.51E-2	5.96E-2	5.88E-2	6.04E-2
60	8.26E-2	8.98E-2	1.22E-1	1.67E-1	2.03E-1	1.55E-1	6.88E-2	2.77E-2	1.57E-2	1.39E-2	1.36E-2
80	4.41E-2	4.54E-2	6.78E-1	1.00E-1	1.32E-1	9.52E-2	3.50E-2	1.17E-2	6.55E-3	5.99E-3	5.57E-3
100	2.63E-2	2.62E-2	4.04E-2	6.58E-2	9.37E-2	6.66E-2	1.95E-2	5.91E-3	3.16E-3	3.17E-3	2.75E-3
120	1.67E-2	1.68E-2	2.63E-2	4.68E-2	7.37E-2	4.68E-2	1.15E-2	3.33E-3	1.97E-3	1.77E-3	1.50E-3
140	1.10E-2	1.14E-2	1.78E-2	3.46E-2	5.73E-2	3.39E-2	7.45E-3	1.98E-3	1.17E-3	9.72E-4	9.61E-4
160	8.22E-3	7.73E-3	1.30E-2	2.63E-2	4.81E-2	2.57E-2	4.63E-3	1.19E-3	1.00E-3	6.38E-4	5.89E-4
180	5.85E-3	5.46E-3	1.01E-2	2.36E-2	3.86E-2	1.98E-2	3.07E-3	8.46E-4	4.67E-4	4.16E-4	3.74E-4
200	4.37E-3	4.01E-3	7.36E-3	1.90E-2	3.41E-2	1.45E-2	2.78E-3	5.96E-4	3.03E-4	3.17E-4	2.69E-4
220	3.25E-3	3.27E-3	6.21E-3	1.51E-2	2.86E-2	1.13E-2	1.59E-3	4.19E-4	2.62E-4	2.47E-4	1.62E-4
240	2.66E-3	2.28E-3	4.99E-3	1.27E-2	2.43E-2	8.69E-3	1.24E-3	3.12E-4	2.04E-4	1.73E-4	1.35E-4
260	1.94E-3	2.10E-3	4.40E-3	1.06E-2	2.24E-2	6.63E-3	9.03E-4	2.56E-4	1.44E-4	1.31E-4	1.04E-4
280	1.63E-3	1.75E-3	3.32E-3	9.18E-3	2.00E-2	5.24E-3	6.55E-4	1.88E-4	1.25E-4	1.12E-4	6.73E-5
300	1.37E-3	1.44E-3	2.70E-3	8.16E-3	1.72E-2	4.39E-3	5.35E-4	1.62E-4	1.08E-4	9.49E-5	6.26E-5
320	1.07E-3	1.22E-3	2.32E-3	6.98E-3	1.61E-2	3.71E-3	4.31E-4	1.41E-4	9.26E-5	7.97E-5	5.98E-5
340	8.22E-4	1.03E-3	1.97E-3	6.35E-3	1.42E-2	2.63E-3	3.24E-4	1.17E-4	7.87E-5	6.35E-5	6.24E-5
360	6.53E-4	1.14E-3	1.70E-3	5.43E-3	1.41E-2	2.08E-3	2.57E-4	1.05E-4	6.99E-5	5.89E-5	4.76E-5
380	5.53E-4	7.66E-4	1.15E-3	5.10E-3	1.10E-2	1.88E-3	1.99E-4	9.22E-5	5.96E-5	4.91E-5	4.06E-5
400	5.08E-4	5.79E-4	1.34E-3	4.38E-3	1.03E-2	1.40E-3	1.81E-4	7.55E-5	5.70E-5	3.88E-5	3.23E-5

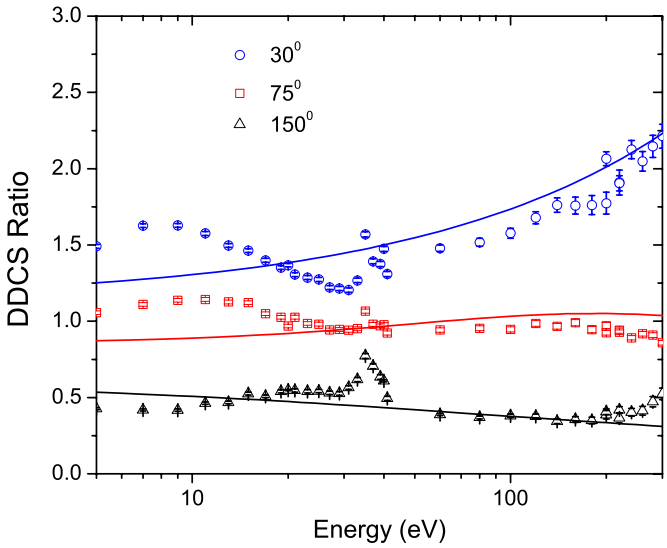

Figure 2. DDCS ratios: symbols represent DDCS ratios of the data with the B1 calculation and the solid curves represent the theoretical ratios between the CDW-EIS and the B1 calculations for three different angles

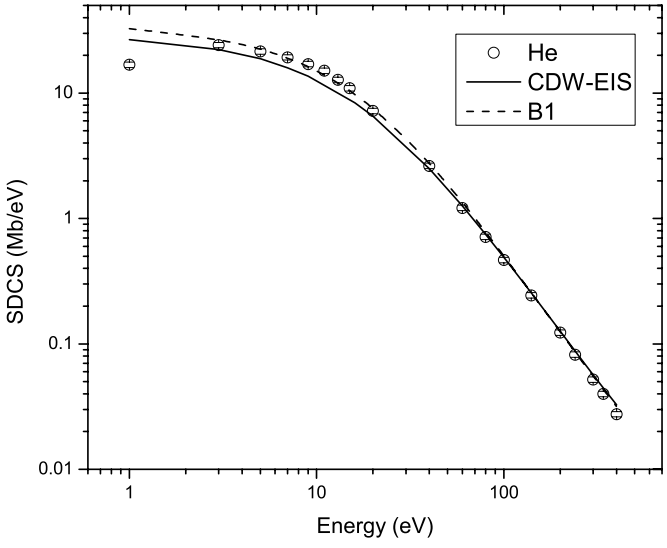

Figure 3. The SDCS as a function of emission energy. The CDW-EIS and B1 calculations are shown as the solid and dashed curves, respectively.

factor over the B1 values is found to vary between 1.5 and 2.0. The agreement with the CDW-EIS is very good, except for the lowest energies, i.e. for less than 10 eV. The ratio is less than unity for 150° angle and is found to be almost 0.5 implying that the experimental values are approximately half of the B1 predicted values. The increasing deviations from unity indicate the enhanced forward emission and reduced emission in the backward direction, as expected by the two-centre model, which predicts the forward focussing. The CDW-EIS seems to provide excellent agreement with the data here. However, the ratio is close to 1 and remains almost constant for the 75° angle, which is highly dominated by the binary-collision process and that is explained by the B1 model. The

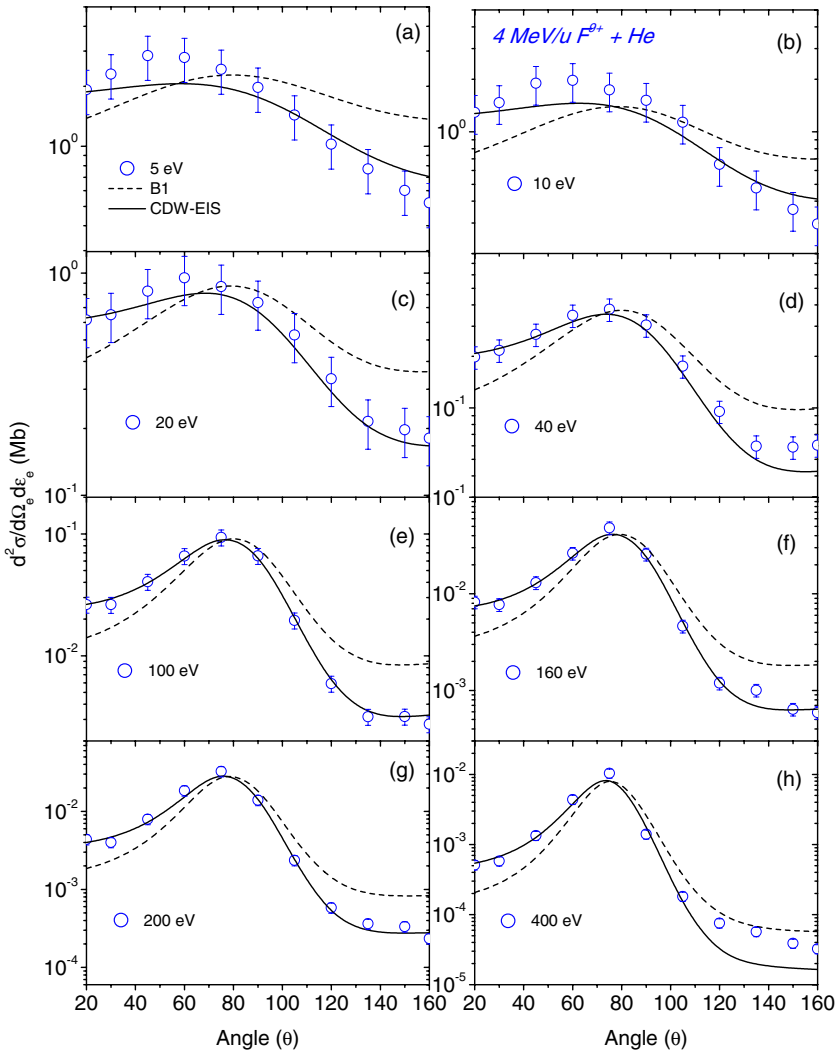

Figure 4. The double-differential cross section of electrons for eight different emission energies, namely, E_e = 5, 10, 20, 40, 100, 160, 200 and 400 eV. The CDW-EIS and B1 calculations are shown as the solid and dashed curves, respectively.

sharp feature around 35 eV energy is due to the decay of the auto-ionizing doubly excited states of the He atom [40, 41].

3.2. Angular distributions at fixed energies

The symbols in figure 4 show the angular distributions of DDCS for several selected electron energies. The CDW-EIS and B1 calculations are shown as the solid and dashed curves, respectively. The angular distributions show a large forward–backward asymmetry due to the TCE, which is not reproduced by the B1, but qualitatively reproduced by the CDW-EIS calculations. As observed, the overall agreement of CDW-EIS calculations is found to be excellent over the entire angular range and for all the energies studied. However, for extreme backward angles and very high energies (figure 4(h)), the CDW-EIS results underestimate the experimental results to some extent and the B1 predictions seem to be in better agreement. However, this behaviour is not quite understood at this stage. For low-energy electrons (up to 40 eV), the B1 calculations completely fail to explain the observed angular distribution. For higher energies, it underestimates at forward angles and overestimates at backward angles. However, the agreement is quite good for angles close to 90°. This can be understood from the fact that most of the electrons emitted close to 90° result from a binary collision between the target electrons and the projectile ions, and hence, the trajectories of the subsequent motion of these electrons are least affected by the receding projectile ion. The B1 calculation considers the target centre effects, and hence, good agreement is obtained.

In figure 5, we show the angular distribution of the SDCS along with the B1 and CDW-EIS predictions. The data show overall excellent agreement with CDW-EIS for the backward angles, whereas a deviation is observed for a few forward emission angles. The B1 predictions largely deviate in both the forward and the backward emission angles. We have also calculated the total cross section from the measured DDCS spectra, which is found to be 491 Mb, and the predictions of CDW-EIS [7, 28] and B1 calculations are 461 and 516 Mb, respectively. The total cross sections are in agreement within 6%.

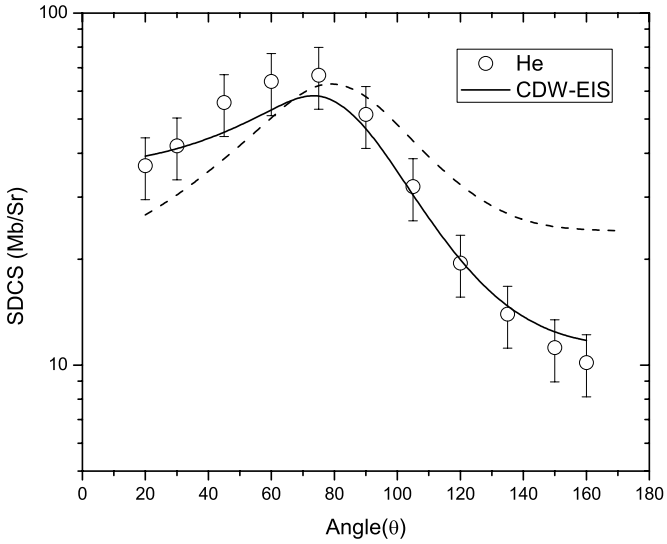

Figure 5. The SDCS of electron emission as a function of emission angle. The CDW-EIS and B1 calculations are shown as the solid and dashed curves, respectively.

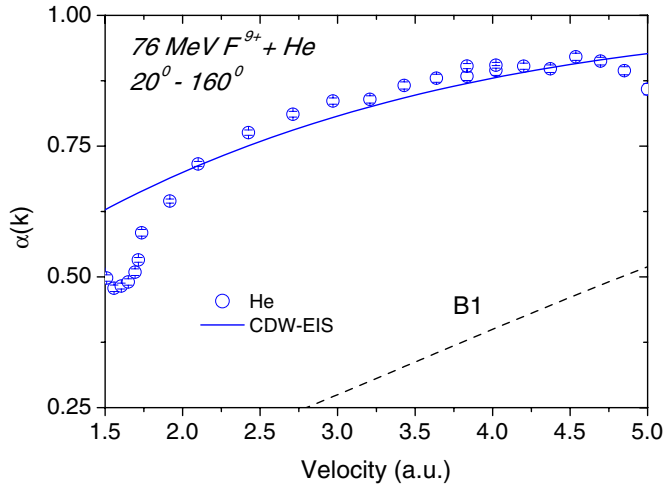

Figure 6. Forward–backward symmetry parameter for 20° and 160°. The CDW-EIS and B1 calculations are shown as the solid and dashed curves, respectively.

3.3. Forward–backward asymmetry parameter

The long-range Coulomb interactions between the emitted electron and the residual target ion, as well as the receding projectile ion, play an important role in the subsequent evolution of the trajectory of the emitted electron. The so-called two-centre effect (TCE) is responsible for the forward focusing of the emitted electrons and results in a large forward–backward asymmetry in the electron emission. Also, for two- or multi-electron targets, such as He, the non-Coulombic nature of the interaction potential has been shown to cause the forward–backward asymmetry in the electron emission [6, 10, 42, 43]. We define the quantity $\alpha(k)$ as

$$\alpha(k,\theta) = \frac{\sigma(k,\theta) - \sigma(k,\pi-\theta)}{\sigma(k,\theta) + \sigma(k,\pi-\theta)}, \qquad (1)$$

where k is the velocity of the ejected electron in au and θ is a small forward angle, e.g., 20°. It has been shown by Fainstein *et al* [44] that $\alpha(k)$ would represent the angular asymmetry parameter by expanding the cross section $\sigma(k,0)$ in terms of Legendre's polynomials. Since angular distributions vary slowly near 0 and π [10], the measured $\alpha(k,20^\circ)$ can be approximately taken as the angular asymmetry parameter. In figure 6, we show the asymmetry parameter as a function of velocity of the ionized electron along with the CDW-EIS and B1 predictions. It is evident from figure 6 that the asymmetry parameter smoothly increases from about 50% to about 85% in the considered velocity range and is in reasonable agreement with the CDW-EIS predictions. However, the B1 predictions largely underestimate the data.

4. Conclusions

We have measured the energy and angular distributions of low-energy electron emission in fast bare F ion collisions with He. We have shown that the measurements of the electron DDCS from He provide crucial information regarding the ionization mechanism. The overall agreement of CDW-EIS calculations is found to be excellent except for extreme backward angles where the theory underestimates the experimental results. The B1 calculation underestimates the cross sections at forward angles, whereas it overestimates the cross sections at backward angles. However, the agreement is found to be good for angles close to 90°, i.e. in the binary-collision-dominated regime. The ratios of experimental DDCS to that predicted by B1 clearly indicate the forward enhancement and the backward depletion. The forward–backward asymmetry parameter has been determined and the energy dependence is well reproduced by the CDW-EIS model, signifying the quantitative estimation of the TCE. Besides the absolute DDCS, we have also derived the SDCSs in terms of angle and electron energy and finally the total cross section. Excellent agreement is found with the CDW-EIS-predicted values for both the SDCS distributions. The derived total cross section agrees with the CDW-EIS and B1 predictions within about 6%. All the data are provided in tabulated form which along with the existing data for different projectiles (although at a few energies) will help to create a database on electron emission from He.

References

[1] Bethe H A 1930 *Ann. Phys., Lpz.* **5** 325
[2] Hooper J W, McDaniel E W, Martin D W and Harmer D S 1961 *Phys. Rev.* **121** 1123
[3] Kuyatt C E and Jorgenson T Jr 1963 *Phys. Rev.* **130** 1444
[4] Moshammer R, Ullrich J, Kollmus H, Schmitt W, Unverzagt M, Schmidt-Bocking H, Wood C J and Olson R E 1997 *Phys. Rev.* A **56** 1351
[5] Ullrich J, Moshammer R, Dörner R, Jagutzki O, Mergel V, Schmidt-Bocking H and Spielberger L 1997 *J. Phys. B: At. Mol. Opt. Phys.* **30** 2917
[6] Stolterfoht N, Platten H, Schiwietz G, Schneider D, Gulyás L, Fainstein P D and Salin A 1995 *Phys. Rev.* A **52** 3796
[7] Fainstein P D, Ponce V H and Rivarola R D 1991 *J. Phys. B: At. Mol. Opt. Phys.* **24** 3091
[8] Kerby G W III, Gealy M W, Hsu Y-Y, Rudd M E, Schultz D R and Reinhold C O 1995 *Phys. Rev.* A **51** 2256

[9] Kerby G W III, Gealy M W, Hsu Y-Y and Rudd M E 1995 *Phys. Rev.* A **51** 2247
[10] Tribedi L C, Richards P, DeHaven W, Gulyás L, Gealy M W and Rudd M E 1998 *J. Phys. B: At. Mol. Opt. Phys.* **31** L369
[11] DuBois R D and Rudd M E 1978 *Phys. Rev.* A **17** 843
[12] Tribedi L C, Richard P, Gulyás L, Rudd M E and Moshammer R 2001 *Phys. Rev.* A **63** 062723
[13] Tribedi L C, Richard P, Gulyás L and Rudd M E 2001 *Phys. Rev.* A **63** 062724
[14] Misra D, Kelkar A H, Kadhane U, Kumar A, Singh Y P, Tribedi L C and Fainstein P D 2007 *Phys. Rev.* A **75** 052712
[15] Lee D H, Richard P, Zouros T J M, Sanders J M, Shinpaugh J L and Hidmi H I 1990 *Phys. Rev.* A **41** 4816
[16] Zouros T J M, Wong K L, Grabbe S, Hidmi H I, Richard P, Montenegro E C, Sanders J M, Liao C, Hagmann S and Bhalla C P 1996 *Phys. Rev.* A **53** 2272
[17] Suárez S, Garibotti C, Meckbach W and Bernardi G 1993 *Phys. Rev. Lett.* **70** 418
[18] Tribedi L C, Richard P, Wang Y D, Lin C D, Olson R E and Gulyás L 1998 *Phys. Rev.* A **58** 3626
[19] Tribedi L C, Richard P, Wang Y D, Lin C D, Gulyás L and Rudd M E 1998 *Phys. Rev.* A **58** 3619
[20] Tribedi L C, Richard P, Wang Y D, Lin C D and Olson R E 1996 *Phys. Rev. Lett.* **77** 3767
[21] Shyn T W 1992 *Phys. Rev.* A **45** 2951
[22] Rudd M E and Zorgensen T Jr 1963 *Phys. Rev.* **131** 666
[23] Rudd M E, Sautter C A and Bailey C L 1966 *Phys. Rev.* **151** 20
[24] Manson S T, Toburen L H, Madison D H and Stolterfoht N 1975 *Phys. Rev.* A **12** 60
[25] Hsu Y-Y, Gealy M W, Kerby G W III and Rudd M E 1996 *Phys. Rev.* A **53** 297
[26] Hsu Y-Y, Gealy M W, Kerby G W III, Rudd M E, Schultz D R and Reinhold C O 1996 *Phys. Rev.* A **53** 303
[27] Crothers D S F and McCann J F 1983 *J. Phys. B: At. Mol. Phys.* **16** 3229
[28] Gulyás L, Fainstein P D and Salin A 1995 *J. Phys. B: At. Mol. Opt. Phys.* **28** 245
[29] Cohen H D and Fano U 1966 *Phys. Rev.* **150** 30
[30] Jain D K and Khare S P 1977 *Phys. Lett.* A **63** 237
[31] Stolterfoht N *et al* 2001 *Phys. Rev. Lett.* **87** 023201
[32] Misra D, Kadhane U, Singh Y P, Tribedi L C, Fainstein P D and Richard P 2004 *Phys. Rev. Lett.* **92** 153201
[33] Frémont F, Hajaji A, Naja A, Leclercq C, Soret J, Tanis J A, Sulik B and Chesnel J-Y 2005 *Phys. Rev.* A **72** 050704
[34] Misra D, Kelkar A H, Kadhane U, Kumar A and Tribedi L C 2006 *Phys. Rev.* A **74** 060701
[35] Chatterjee S, Misra D, Kelkar A H, Fainstein P D and Tribedi L C 2010 *J. Phys. B: At. Mol. Opt. Phys.* **43** 125201
[36] Galassi M E, Rivarola R D, Fainstein P D and Stolterfoht N 2002 *Phys. Rev.* A **66** 052705
[37] Stolterfoht N *et al* 1987 *Europhys. Lett.* **4** 899
[38] Narvekar S D, Hosangdi R R, Tribedi L C, Pillay R G, Prasad K G and Tandon P N 1992 *Pramana J. Phys.* **39** 79
[39] Misra D, Thulasiram K V, Fernandez W, Kelkar A H, Kadhane U, Singh Y P, Kumar A and Tribedi L C 2009 *Nucl. Instrum. Methods* B **267** 157
[40] Compton K T and Boyce J C 1928 *J. Franklin Inst.* **205** 497
[41] Kruger P G 1930 *Phys. Rev.* **36** 855
[42] Pedersen J O P, Hvelplund P, Petersen A and Fainstein P D 1991 *J. Phys. B: At. Mol. Opt. Phys.* **24** 4001
[43] Suárez S, Garibotti C, Meckbach W and Bernardi G 1993 *Phys. Rev. Lett.* **70** 418
[44] Fainstein P D, Gulyás L, Martin F and Salin A 1996 *Phys. Rev.* A **53** 3243